ANTIMICROBIAL AGENTS AND CHEMOTHERAPY, July 2005, p. 2589–2597 Vol. 49, No. 7
0066-4804/05/$08.00+0 doi:10.1128/AAC.49.7.2589–2597.2005

Pharmacology and Pharmacokinetics of the Antiviral Agent β-D-2′,3′-Dideoxy-3′-Oxa-5-Fluorocytidine in Cells and Rhesus Monkeys†

Brenda I. Hernandez-Santiago,[1] Huachun Chen,[1] Ghazia Asif,[1] Thierry Beltran,[1] Shuli Mao,[2] Selwyn J. Hurwitz,[1] Jason Grier,[1] Harold M. McClure,[3] Chung K. Chu,[2] Dennis C. Liotta,[4] and Raymond F. Schinazi[1]*

Department of Pediatrics, Emory School of Medicine/Veterans Affair Medical Center,[1] Yerkes National Primate Center,[3] and Department of Chemistry, Emory University,[4] Decatur, Georgia 30033, and College of Pharmacy, University of Georgia, Athens, Georgia 30602[2]

Received 7 December 2004/Returned for modification 8 February 2005/Accepted 3 March 2005

β-D-2′,3′-Dideoxy-3′-oxa-5-fluorocytidine (D-FDOC) is an effective inhibitor of human immunodeficiency virus 1 (HIV-1) and HIV-2, simian immunodeficiency virus, and hepatitis B virus (HBV) in vitro. The purpose of this study was to evaluate the intracellular metabolism of D-FDOC in human hepatoma (HepG2), human T-cell lymphoma (CEM), and primary human peripheral blood mononuclear (PBM) cells by using tritiated compound. By 24 h, the levels of D-FDOC-triphosphate (D-FDOC-TP) were 2.8 ± 0.4, 6.7 ± 2.3, and 2.0 ± 0.1 pmol/10^6 cells in HepG2, CEM, and primary human PBM cells, respectively. Intracellular D-FDOC-TP concentrations remained greater than the 50% inhibitory concentration for HIV-1 reverse transcriptase for up to 24 h after removal of the drug from cell cultures. In addition to D-FDOC-monophosphate (D-FDOC-MP), -diphosphate (D-FDOC-DP), and -TP, D-FDOC-DP-ethanolamine and D-FDOC-DP-choline were detected in all cell extracts as major intracellular metabolites. D-FDOC was not a substrate for *Escherichia coli* thymidine phosphorylase. No toxicity was observed in mice given D-FDOC intraperitoneally for 6 days up to a dose of 100 mg/kg per day. Pharmacokinetic studies in rhesus monkeys indicated that D-FDOC has a $t_{1/2}$ of 2.1 h in plasma and an oral bioavailability of 38%. The nucleoside was excreted unchanged primary in the urine, and no metabolites were detected in plasma or urine. These results suggest that further safety and pharmacological studies are warranted to assess the potential of this nucleoside for the treatment of HIV- and HBV-infected individuals.

Forty-thousand new cases of human immunodeficiency virus type 1 (HIV-1) infection are reported each year, and more than 40 million people are infected worldwide with the HIV-1 (19). Currently, highly active antiretroviral therapy for chronically infected patients with HIV-1 may be suboptimal due to low response rates related to drug-toxicity, imperfect compliance, and/or the development of resistant virus. The large viral turnover and high error rate of HIV-1 reverse transcriptase (RT) can cause the rapid selection of drug-resistant viral strains in vitro and in vivo (24, 29).

There is a need for salvage drug therapy effective against viruses that are resistant to all classes of drugs, especially zidovudine and lamivudine. The only other nucleoside analogue commonly used for salvage therapy, tenofovir disoproxil fumarate, is not effective against viruses containing two or more thymidine-associated mutations or when the K65R mutation is selected or present in vivo (16).

The potency and selectivity of a new antiretroviral agent, β-D-2′,3′-dideoxy-3′-oxa-5-fluorocytidine (D-FDOC), against wild-type and drug-resistant viruses in vitro warranted further studies on this nucleoside analogue (14). D-FDOC is an effective inhibitor of HIV-1, HIV-2, simian immunodeficiency virus, and hepatitis B virus in vitro. The 50% effective concentration (EC_{50}) and EC_{90} of D-FDOC in primary human lymphocytes infected with $HIV\text{-}1_{LAI}$ were 0.04 and 0.26 μM, respectively. D-FDOC showed minimal toxicity in various systems, including no increase in lactic acid production at 300 μM and no inhibition of mitochondrial DNA synthesis up to a concentration of 10 μM (22).

The objectives of the in vitro studies included: to describe the cellular metabolism of D-FDOC in human T-cell lymphoma (CEM), peripheral blood mononuclear (PBM), and human hepatoma (HepG2) cell lines; measurement of the cellular decline rates of D-FDOC metabolites in primary human PBM and HepG2 cells; D-FDOC was also evaluated as a potential substrate for *Escherichia coli* thymidine phosphorylase to ensure that this nucleoside is not metabolized by this ubiquitous enzyme. The in vivo objectives of the present study included toxicity screening of D-FDOC in mice and determination of the single-dose pharmacokinetics of D-FDOC in rhesus monkeys after oral and intravenous (i.v.) administration.

MATERIALS AND METHODS

Chemicals. D-FDOC was synthesized in our laboratory and purified by chiral HPLC as previously reported (14). [6-^{3}H]-D-FDOC (specific activity = 8.6 Ci/mmol) was custom synthesized by Moravek Biochemicals, Inc. (Brea, CA). Tetrabutylammonium phosphate (TBAP) was purchased from Alltech Assoc., Inc.

* Corresponding author. Mailing address: Veterans Affairs Medical Center, Medical Research 151H, 1670 Clairmont Rd., Decatur, GA 30033. Phone: (404) 728-7711. Fax: (404) 728-7726. E-mail: rschina@emory.edu.

† Dedicated to the memory of Harold M. McClure (1937–2004), our coauthor, colleague, and dear friend.

(Deerfield, IL). Scintillation liquid, EcoLite, was obtained from Valeant Pharmaceuticals (Costa Mesa, CA). The chemical purity of each compound, as determined by high-performance liquid chromatography (HPLC) and spectral analysis, was >98%. Methanol (HPLC grade), and all other chemicals (analytical grade) were obtained from Fisher Scientific (Fair Lawn, N.J.).

Cell culture systems. The human hepatocellular carcinoma cell line, HepG2, was obtained from American Type Culture Collection (ATCC; Rockville, MD) and maintained in a 75-cm^2 flask in Dulbecco modified Eagle medium supplemented with 4.5 g of glucose (MediaTech, Inc., Herndon, VA)/liter, 10% (vol/vol) heat-inactivated fetal bovine serum (FBS), and 1 mM penicillin G-streptomycin sulfate. CEM cells were obtained from the ATCC and were maintained in suspension culture in RPMI 1640 medium (Gibco Laboratories, Grand Island, NY), supplemented with 1 mM sodium pyruvate, 10% (vol/vol) FBS, and 1 mM penicillin G-streptomycin sulfate. All cell lines were grown at 37°C in a 5% CO_2–95% air atmosphere. The medium was replenished every 3 days, and cells were subcultured once a week.

PBM cells were isolated by using a Histopaque technique from buffy coats derived from healthy donors (samples were obtained from the American Red Cross in Atlanta, GA). After processing, the PBM cells were stimulated by incubating cells for 2 to 3 days in medium containing 10 μl of phytohemagglutinin (PHA)/ml.

The medium used in the accumulation and decay studies were supplemented with 10% FBS. Protein-binding studies were not performed since nucleoside RT inhibitors do not typically demonstrate significant binding to serum proteins.

Accumulation studies. HepG2 cells (1.5×10^6 cells per time point) and CEM and PHA-activated primary human PBM cells (10^7 cells per time point) were suspended in a final volume of 1.5 or 10 ml of medium supplemented with 10% FBS and exposed to 10 μM [^{3}H]-D-FDOC (1,000 dpm/pmol) at 1, 2, 4, 8, and 24 h. The cells were maintained at 37°C under a 5% CO_2 atmosphere. Intracellular metabolites were extracted as described below.

Determination of intracellular D-FDOC-triphosphate (D-FDOC-TP) half-life. HepG2 cells were plated at a density of 1.5×10^6 per well in a six-well plate, and PBM cells were plated at 10^7 cells per 25-cm^2 flask. The cells were incubated with 10 μM [^{3}H]-D-FDOC (1,000 dpm/pmol) for a period of 24 h at 37°C in a 5% CO_2 atmosphere. The cells were then washed three times with drug-free medium to remove extracellular D-FDOC and incubated with regular culture medium for specific time periods (0, 1, 2, 4, 8, and 24 h). Intracellular metabolites were extracted as described below.

Determination of intracellular metabolites in CEM and activated primary human PBM cells. At selected times of accumulation or decay studies, the cells were centrifuged for 10 min at $350 \times g$ at 4°C, and the pellet was resuspended and washed three times with cold phosphate-buffered saline. Viable cells were counted by using a hemocytometer, and the viability was assessed by trypan blue exclusion (viability > 98%). D-FDOC and its respective metabolites were extracted by incubation overnight at −20°C with 60% methanol-water (1 ml), the supernatants were then collected and centrifuged at 14,000 rpm (Eppendorf centrifuge model 5415C) for 5 min. The pellets were then reextracted for 1 h on ice by using an additional 200 μl of 60% methanol in water, followed by centrifugation at 14,000 rpm for 5 min. The extracts were then combined, dried under a gentle filtered airflow, and stored at −20°C until they were assayed. The residues were resuspended in 200 μl of water, and aliquots were injected into the HPLC system (below).

Determination of intracellular metabolites in HepG2 cells. At selected times of accumulation or decay studies, the extracellular medium was removed, and the cell layer washed three times with phosphate-buffered saline. Then, 1 ml of 60% methanol in water (1 ml) was added, and the cells were scraped off the surface. The suspension of cell debris was extracted, and the metabolites of D-FDOC were assayed as described above for CEM and PBM cells.

HPLC analysis of intracellular metabolites. D-FDOC and their respective metabolites were separated by reversed-phase HPLC with a Columbus 5-μm C_{18} column (250 by 4.6 mm; Phenomenex, Torrance, CA) on a Varian ProStar HPLC model 210 by using a manual injector (Varian, Walnut Creek, CA). The mobile phase consisted of buffer A (25 mM ammonium acetate with 5 mM TBAP [pH 7.0]) and buffer B (methanol). Elution was performed by using a multistage linear gradient of buffer B from 0 to 40%. Radioactivity was quantified by using a 2500 TR liquid scintillation analyzer (Perkin-Elmer/Life and Analytical Sciences, Wellesly, MA).

LC-MS analysis. The liquid chromatography-tandem mass spectrometry (LC/MS/MS) system was equipped with a Waters LC (controller 600 and UV photodiode array detector 996) coupled to a Finnigan TSQ mass spectrometer (ThermoQuest, San Jose, CA) equipped with an electrospray ionization (ESI) source. The analytical column was a C_{18} X-terra column (4.6 by 150 mm, 3.5 μm; Waters). The composition of mobile phase A was 50 mM triethylammonium formate (pH 8), and mobile phase B contained 50 mM triethylammonium formate (pH 8) with 20% methanol. The flow rate was 0.5 ml/min. The mass spectrometer was operated in ESI-positive ion mode. Nitrogen was used as both the sheath and auxiliary gas at pressures of 80 and 20 U, respectively. The spray voltage and the capillary temperature were set at 4.5 kV and 300°C, respectively. The D-FDOC nucleoside and metabolites were first detected in the medium by using full-scan MS in Q1. Full-scan MS/MS was then performed for each analyte to obtain structural confirmations. Collision-induced dissociation of the parent ions was performed in the collision cell (Q2) with argon gas at 1.5 torr and with the collision energy optimized at 30 eV, producing the highest abundance of product ions in Q1. Subsequent product ions generated from the collision of the Q1 ions with collision gas in Q2 were selected by the third quadrupole (Q3) for identification.

Thymidine phosphorylase assay. The standard reaction mixtures contained 10 μM [^{3}H]-D-FDOC in 100 mM KH_2PO_4, (pH 7.4) at room temperature. The reaction was initiated by adding 1.1 U of thymidine phosphorylase enzyme (*E. coli*, Sigma catalog no. T-2807) to a final volume of 200 μl. Reactions were incubated at room temperature and terminated by filtering through a 0.45-μm-pore-size Acrodisc LC13 polyvinylidene difluoride filter (Gelman Sciences, Ann Arbor, MI) at 30 and 60 min after addition of the enzyme. The eluent was frozen at −70°C until HPLC analysis.

Samples were analyzed by HPLC using a Hypersyl ODS-18 5-μm column (Phenomenex) using a Pro Star 210 model with manual injection (Varian). The mobile phase consisted of buffer A (10 mM KH_2PO_4 [pH 6.6]) and buffer B (methanol). The method consisted of an isocratic elution for 5 min with 10 mM KH_2PO_4 and then a 10-min linear gradient from 0 to 30% methanol (23). Radioactivity was measured by using a 500TR Radiometric Flo-One radiochromatography analyzer (Perkin-Elmer/Life and Analytical Sciences).

Toxicity determination in mice. Acclimatized 6-week-old female Swiss mice (SWR/J; Charles River Laboratory, Wilmington, Mass.) were treated intraperitoneally (i.p.) with 300 μl of D-FDOC dissolved in pyrogen-free, sterile 0.85% NaCl solution at doses of 0, 3, 10, 33, or 100 mg/kg of body weight/day for 6 days. Animals were monitored daily for weight (loss or gain), ruffled fur, and mortality for up to 24 days after the end of treatment as previously described (26). All experiments were conducted under the approval of the Institutional Animal Care and Use Committee of the Department of Veterans Affairs, Atlanta, GA.

Monkey studies. Three rhesus monkeys (*Macaca mulatta*, two male and one female) weighing from 5.4 to 9.4 kg were used for the pharmacokinetic studies. The animals were maintained at the Yerkes National Primate Research Center (Emory University, Atlanta, GA), which is fully accredited by the American Association for Accreditation of Laboratory Animal Care, in accordance with guidelines established by Animal Welfare Act and the Guide for the Care and Use of Laboratory Animals of the National Institutes of Health. Animals were given 33.3 mg/kg by i.v. and oral routes. The i.v. dose was administered in saline, and the oral dose was given by gastric intubations, in a total volume of 10 ml of water, followed by a further 3 ml of water. Oral and i.v. doses were administered 5 weeks apart. Animals were maintained under anesthesia for 4 h after dosing with a mixture of ketamine HCl (60 mg) and tiletamine HCl plus zolazepam HCl (Telazol; 20 mg) intramuscularly and were monitored for alertness. Additional anesthesia (30 to 60 mg of ketamine HCl) was given when necessary. Animals were maintained on their sides on a warm heating pad and were covered with a blanket. Blood samples were taken prior to and at 0.25, 0.5, 1, 1.5, 2, 3, 4, 6, 8, and 24 h after drug administration through the femoral vein while the animals were lying on their backs. Additional 12 h samples were taken for two animals after i.v. and one animal after oral administration of D-FDOC. Cerebrospinal fluid (CSF) samples were taken from all treated monkeys at 1 h after drug administration by cisternal or lumbar tap with a 22-gauge needle. The monkeys were catheterized for urine collection. Urine samples were collected at 0 to 0.25, 0.25 to 0.5, 0.5 to 1, 1 to 1.5, 1.5 to 2, 2 to 3, 3 to 4, 4 to 6, 6 to 8, and 24 h after dosing. Plasma, CSF, and urine samples were frozen at −70°C until analysis.

HPLC analysis of D-FDOC in monkey plasma, urine, and CSF samples. D-FDOC was assayed by using a Hitachi HPLC system (Tokyo, Japan) equipped with a model L-7100 pump, a model L-7400 detector, and a model L-7200 autosampler with a Columbus C_{18} column (4.6 by 250 mm; 5 μm). Thymidine was used as an internal standard. The mobile phase was acetonitrile and water. The mobile phase was a linear gradient from 100% water to 85% water and 15% acetonitrile in 12 min; this phase was then held for 3 min before it was changed to 100% water. The flow rate was maintained at 1 ml/min. D-FDOC and thymidine were detected at a UV wavelength of 238 nm and eluted at 12 and 14 min, respectively.

Preparation of standards for HPLC. Standard solutions of D-FDOC were prepared using water. Calibration plots for D-FDOC in plasma were prepared by adding standard solutions to blank plasma at concentrations ranging from 0.1 to

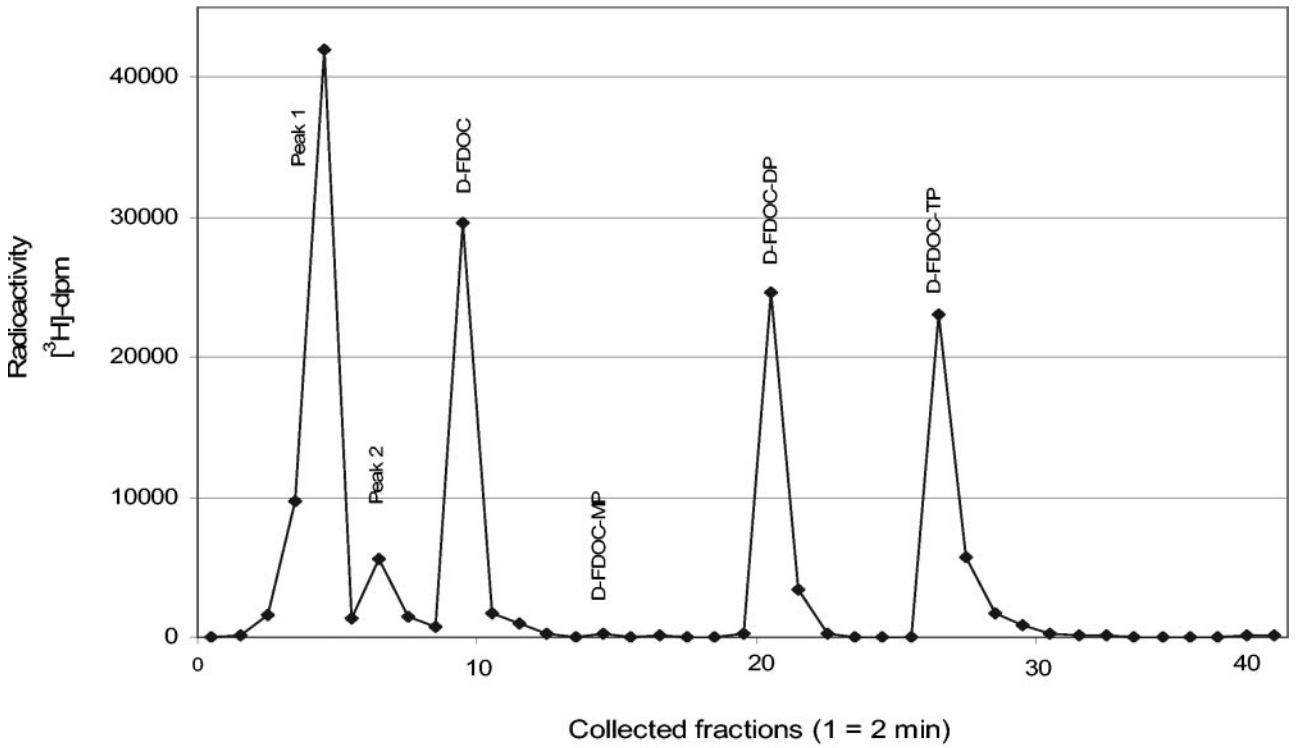

FIG. 1. HPLC radiochromatogram of intracellular extracts from PBM cells incubated with 10 μM [^{3}H]-D-FDOC for 24 h. Metabolites were separated by reversed-phase HPLC with a Columbus 5-μm C_{18} column (Phenomenex) using a model Pro Star (Varian) with manual injection. The mobile phase consisted of buffer A (25 mM ammonium acetate with 5 mM TBAP [pH 7.0]) and buffer B (methanol). Elution was performed by using a multistage linear gradient of buffer B.

100 μg/ml. Standard curves for the analysis of urine and CSF samples were prepared in urine and water, respectively, over the same concentration range.

Five hundred microliters of acetonitrile was added to a 50-μl plasma sample in a microcentrifuge tube, and 40 μl of thymidine at 200 μg/ml was added as an internal standard, followed by vortexing and centrifugation at 11,200 × *g* for 5 min. The supernatant was evaporated to dryness, and the samples were reconstituted with 200 μl of 5% acetonitrile and injected onto the HPLC column. For CSF samples, 20 μl of thymidine solution (200 μg/ml) was added to 100 μl of CSF samples, and the mixtures were injected onto the HPLC column for analysis. Urine samples were diluted 50- to 100-fold, and 20 μl of the thymidine solution was added to 100 μl of diluted urine before injection (25 to 50 μl) onto an HPLC column. The percent recovery of D-FDOC in the assay was >90%, and the limit of detection for the assay was 0.1 μg/ml. The inter- and intraday variance was <10%.

Pharmacokinetic analysis. The concentration in plasma versus time data after i.v. and oral administration were simultaneously fitted for each animal to a two-compartment open pharmacokinetic model by using a nonlinear regression curve-fitting program (WinNonlin, version 4.01; Pharsight Corp., Mountain View, CA). This approach is useful when both sets of data are available from the same animal, since it avoids reporting two different sets of disposition rate constants for the same animal. In addition to intercompartmental disposition rate constants, the fit also estimated the oral absorption rates (K_a) and the fraction of drug absorbed (F) (7). There was no evidence of an appreciable lag time before the onset of oral absorption. Initial estimates for model parameters were obtained using parameters from similar compounds tested in rhesus monkeys. The adequacy of model fit was assessed by examining the overall dispersion of data over the predicted curves and predicted standard errors of the fitted parameters. The model parameters fitted (see Table 2) and the fit of the model to the plasma data (see Fig. 3) were determined. Accurate urine volumes were not available for the oral dose interval between 8 and 24 h. Therefore, the fraction of total dose excreted in the urine (F_e) was derived indirectly, together with the renal clearance (CL_R), by simultaneously fitting the urinary excretion rate (dX_u/dt) concomitantly to the model predicted plasma concentrations (C_p) by using nonweighted least-squares nonlinear regression. The equation used was $dX_u/dt = CL_R \cdot C_p$, where C_p is the predicted plasma concentration using the plasma data (see above), coinciding with the midpoint of the urine collection interval and X_u is the amount of compound recovered from the urine during that collection interval (3). Fitting i.v. and oral data simultaneously assumes a constant renal clearance for both routes of administration. This method is considered robust and does not require measurement of the total amount excreted in the urine or complete bladder emptying within all sampled intervals or urine collection over short intervals relative to the half-life of the drug (7). Peak concentrations in plasma (C_{max}) and the corresponding times (T_{max}) were reported as the observed concentrations and times of maximal concentration after oral administration. The area under the plasma concentration-time curve (AUC) from time zero to infinity for both routes of administration ($AUC_{0-\infty}$) was calculated as $AUC_t + C_t/\beta$, where β is the terminal rate constant of elimination. AUC_t was calculated by using the linear trapezoidal rule, and C_t/β is the extrapolation to infinity. The fraction of oral dose absorbed was also estimated as the ratio of $AUC_{0-\infty}$ for the oral and i.v. doses and found to be similar to the model fitted value of F.

RESULTS

HPLC analysis of D-FDOC and characterization of unknown metabolites. D-FDOC is rapidly phosphorylated to its monophosphate, diphosphate, and triphosphate forms. Two other metabolites were also detected (Fig. 1). Both peaks (peaks 1 and 2) were resistant to catabolism with alkaline phosphatase digestion, indicating no terminal phosphate group.

One of the unknown metabolites (peak 1) was characterized by LC/ESI/MS as D-FDOC-diphosphate (DP)-ethanolamine. Two signals were observed in the full-scan mode. The retention times were 2.5 and 34.4 min, with masses (*m*/*z*) of 435 and 232

TABLE 1. Uptake of 10 μM [^{3}H]-D-FDOC (1,000 dpm/pmol) in CEM, PBM, and HepG2 cells

Time (h)	Cell line	Mean intracellular concn (pmol/10^6 cells) ± SD[a]				
		D-FDOC-DP-ethanolamine	D-FDOC-DP-choline	D-FDOC-MP	D-FDOC-DP	D-FDOC-TP
1	CEM	0.6 ± 0.0	2.9 ± 0.6	0.2 ± 0.1	1.9 ± 0.3	1.6 ± 0.2
	PBM	0.3 ± 0.0	0.1 ± 0.0	0.02 ± 0.01	0.2 ± 0.0	0.1 ± 0.0
	HepG2	1.1 ± 0.2	0.6 ± 0.2	0.2	0.7 ± 0.3	0.2 ± 0.1
2	CEM	3.2 ± 0.1	0.13 ± 0.05	0.3 ± 0.1	2.4 ± 0.2	2.9 ± 0.2
	PBM	0.7 ± 0.1	0.1 ± 0.0	ND	0.4 ± 0.0	0.3 ± 0.0
	HepG2	1.6 ± 0.6	1.1 ± 0.0	0.1	0.6 ± 0.2	0.5 ± 0.1
4	CEM	4.4 ± 0.9	3.4 ± 0.7	0.4 ± 0.0	6.4 ± 0.6	8.2 ± 0.6
	PBM	1.4 ± 0.4	0.2 ± 0.1	ND	0.8 ± 0.2	0.8 ± 0.2
	HepG2	3.2 ± 0.7	1.3 ± 0.3	0.3 ± 0.1	1.2 ± 0.1	1.3 ± 0.1
8	CEM	13.2 ± 2.5	4.7 ± 3.1	0.5 ± 0.1	11.0 ± 3.7	13.7 ± 4.9
	PBM	2.5 ± 0.5	0.5	ND	1.5 ± 0.3	1.6 ± 0.2
	HepG2	3.7 ± 0.9	2.4 ± 0.1	ND	1.5 ± 0.1	1.7 ± 0.1
24	CEM	17.8 ± 5.6	16.0 ± 9.4	0.7 ± 0.1	11.3 ± 3.0	6.7 ± 2.3
	PBM	4.0 ± 0.5	0.5 ± 0.1	0.013 ± 0.005	1.8 ± 0.2	2.0 ± 0.1
	HepG2	7.2 ± 2.3	4.1 ± 0.8	0.1	3.7 ± 0.2	2.8 ± 0.4

[a] Values are means of three independent experiments. MP, monophosphate; DP, diphosphate; ND, not detected (limit of detection of ~0.05 pmol/10^6 cells).

Da, respectively. The second signal corresponded to the parent nucleoside (D-FDOC), while the first appeared to be the DP derivative with an additional ethanolamine on the pyrophosphate moiety. This was supported by the fragmentation of the parent ion (*m/z* 435), yielding two daughter ions, 105 and 187 Da, corresponding to the sugar moiety and the pyrophosphate derivative with ethanolamine, respectively. Based on previous work with other cytidine analogues and authentic standards,

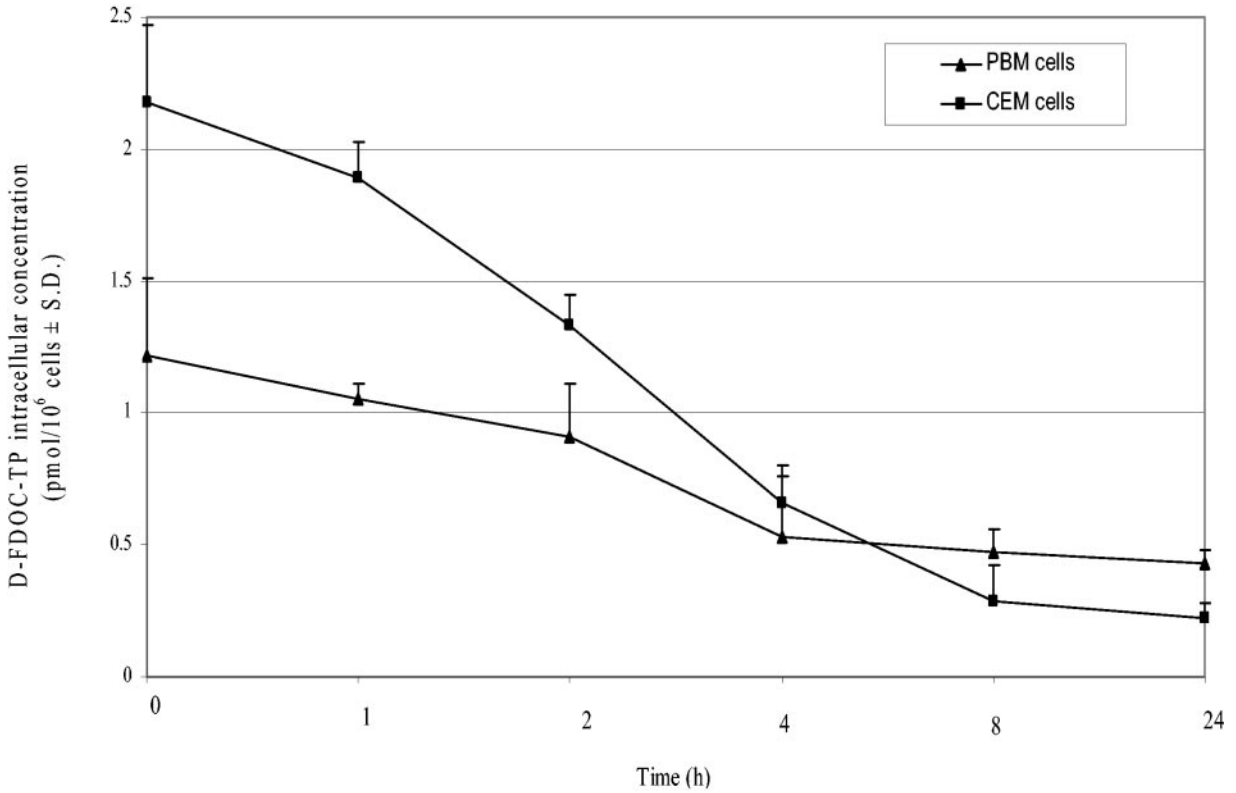

FIG. 2. Egress study of D-FDOC-TP: 10 μM [^{3}H]-D-FDOC (1,000 dpm/pmol) in HepG2 and PBM cells after 24 h of incubation. D-FDOC-TP $t_{1/2}$ values in HepG2 and PBM cells were 2.7 ± 0.8 and 5.7 ± 1.4 h, respectively. The exponential rates of decline (k) for D-FDOC-TP were calculated as the slope of the natural logarithm of the respective concentrations versus time using the terminal linear portion of the curve. The half-life of decay was determined as $-0.693/k$.

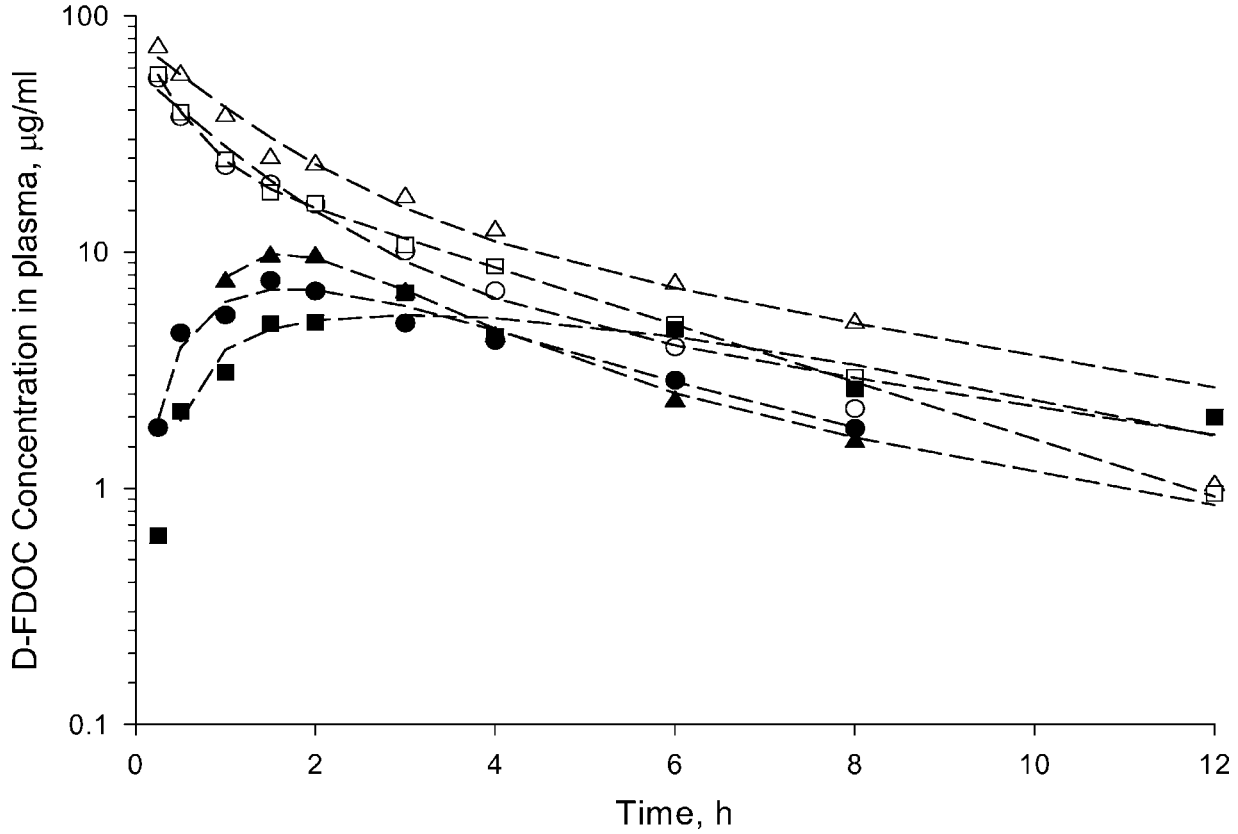

FIG. 3. Observed (symbols) and model-predicted (lines) plasma concentrations of D-FDOC versus time profiles in rhesus monkeys after the administration of 33.3 mg of compound/kg by the i.v. (open symbols) and oral (solid symbols) routes. (Please refer to the text.) To convert micrograms/milliliter concentrations to molar concentrations, values were multiplied by 4.3.

peak 2 was identified as the diphosphocholine nucleoside derivative (10, 15, 18).

Accumulation studies. [^{3}H]-D-FDOC was phosphorylated rapidly to its derivatives in CEM, primary human PBM, and HepG2 cells. The amounts of D-FDOC nucleotides per 10^6 CEM cells were greater than those observed for 10^6 HepG2 and primary human PBM cells. The intracellular concentrations of D-FDOC-TP in CEM, primary human PBM, and HepG2 cells after 24 h of incubation with D-FDOC were 6.7 ± 2.3, 2.0 ± 0.1, and 2.8 ± 0.4 pmol/10^6 cells, respectively (Table 1). The D-FDOC-DP-ethanolamine intracellular concentrations after 24 h of incubation in CEM, primary human PBM, and HepG2 cells with D-FDOC were 17.8 ± 5.6, 4.0 ± 0.5, and 7.2 ± 2.3 pmol/10^6 cells, respectively (Table 1). Another metabolite, D-FDOC-DP-choline, attained intracellular levels of 16.0 ± 9.4, 0.5 ± 0.1, and 4.1 ± 0.8 pmol/10^6 cells in CEM, primary human PBM, and HepG2 cells, respectively, after 24 h of incubation with D-FDOC.

Determination of D-FDOC-TP half-life in human cells. The intracellular half-lives of D-FDOC-TP in HepG2 and primary human PBM cells were 2.7 ± 0.8 and 5.7 ± 1.4 h, respectively (Fig. 2). The intracellular concentrations of D-FDOC-TP remained 55- and 112.5-fold, respectively, greater than the 50% inhibitory concentration (IC_{50}) for the HIV-1 RT for up to 24 h after removal of the drug from these two cell cultures (11, 22).

Effect of *E. coli* thymidine phosphorylase on D-FDOC. D-FDOC was examined for the ability to be cleaved across the glycosidic bond by *E. coli* thymidine phosphorylase. Decreased susceptibility for cleavage by this enzyme was previously reported to be as follows: uridine > thymidine ≫ cytidine (23). Thymidine, used as a positive control, was cleaved 100% by *E. coli* thymidine phosphorylase after 30 min, whereas β-D-2′,3′-dideoxycytidine (ddC), used as a negative control, was not a substrate. D-FDOC was not cleaved by *E. coli* thymidine phosphorylase enzyme when incubated at 37°C for up to 60 min.

Toxicity evaluation for D-FDOC in mice. To determine the potential toxicity of D-FDOC in small animals prior to studies in nonhuman primates, five groups of six 6-week-old female Swiss mice (SWR/J) were given i.p. doses of 0, 3, 10, 33, or 100 mg/kg per day for 6 days. All of the animals survived the 6-day treatment and the 24-day posttreatment monitoring period. The mice were weighed daily for 6 days and then every 2 days until day 30. No statistically significant changes in weight were observed in any of the groups during the treatment period (data not shown). At the end of the treatment period (day 5), their weights were similar to those of mice in the no-drug control group. The no-observed-effect dose level for D-FDOC in this experiment was >100 mg/kg per day.

Pharmacokinetic studies in rhesus monkeys. The disposition of D-FDOC in plasma, CSF, and urine was studied in three rhesus monkeys given oral and i.v. doses of 33.3 mg of D-

TABLE 2. Pharmacokinetic parameters of D-FDOC after i.v. and oral administration of D-FDOC (33.3 mg/kg) to rhesus monkeys

Route and parameter[a]	Value in monkey (gender):			
	1 (M)	2 (F)	3 (M)	Mean ± SD
Two-compartment parameters				
$t_{1/2\alpha}$ (h)	0.26	0.77	0.80	0.61 ± 0.03
$t_{1/2\beta}$ (h)	2.48	5.12	4.53	4.04 ± 1.38
K_{10} (h^{-1})	0.75	0.49	0.44	0.56 ± 0.16
K_{12a} (h^{-1})	1.18	0.29	0.28	0.58 ± 0.51
K_{21} (h^{-1})	0.98	0.25	0.30	0.51 ± 0.41
V_c (liter/kg)	0.38	0.57	0.42	0.46 ± 0.10
V_{ss} (liter/kg)	0.84	1.24	0.80	0.96 ± 0.24
CL_T (liter/h/kg)	0.28	0.28	0.18	0.25 ± 0.06
CL_R (liter/h/kg)	0.19	0.24	0.10	0.18 ± 0.08
$AUC_{i.v.}$ (μg h/ml)	117.4	119.1	182.2	139.6 ± 36.9
$MRT_{i.v.}$ (h)	2.95	4.43	4.39	3.92 ± 0.85
r^2 (observed vs predicted i.v.)	0.999	0.975	0.983	0.99 ± 0.01
CSF (1 h, μg/ml)	1.62	1.75	2.35	1.90 ± 0.40
Parameters specific for oral routes				
K_{at} (h^{-1})	0.85	0.49	0.22	0.52 ± 0.32
F (%)	0.28	0.39	0.48	0.38 ± 0.10
T_{lag} (h)	0.25	0.07	0.50	0.27 ± 0.22
AUC_{oral} (μg h/ml)	52.32	45.47	46.89	48.23 ± 3.62
r^2 (observed vs predicted oral)	0.830	0.954	0.997	0.93 ± 0.09
C_{max} (observed) (μg/ml)	6.70	9.55	7.56	7.94 ± 1.46
T_{max} (observed) (h)	3.0	1.5	1.5	2.00 ± 0.87
CSF (1 h, μg/ml)	0	0.17	0.11	0.09 ± 0.09

[a] V_C, distribution volume of central compartment; $t_{1/2\alpha}$ and $t_{1/2\beta}$, half-lives of biexponential decay in plasma ($t_{1/2\alpha} < t_{1/2\beta}$); k_{12a} and k_{21}, disposition rate constants describing movement between the central and peripheral compartments; k_{10}, the elimination rate constant for the central compartment; $AUC_{i.v.}$, area under plasma concentration-time curve; F (%), percent oral dose absorbed; AUC_{oral}, AUC after oral dose = $F \cdot AUC_{i.v.}$; $MRT_{i.v.}$, mean residence time after i.v. dosing; V_{ss}, steady-state distribution volume; C_{max} and T_{max}, observed peak concentrations in plasma and time of maximum concentration after dose respectively; CL_R, renal clearance; CL_T, systemic clearance; T_{lag}, time between dosing and onset of oral absorption; K_{at}, absorption rate constant; CSF, cerebrospinal fluid; r^2, correlation between the predicted values using the model and the observed values.

FDOC/kg. The observed concentrations in plasma and fitted curves versus time for the i.v. and oral routes of administration are shown in Fig. 3, and the model parameters for individual monkeys and pooled data are shown in Table 2. Plasma concentrations declined in a biexponential manner after i.v. administration with an average systemic clearance (CL_T) of 0.25 liter · h^{-1} · kg^{-1} and a terminal phase half-life of 4.04 h. The mean distribution volume of the central compartment was 0.46 liter · kg^{-1}, and the steady-state distribution volume was 0.96 liter · kg^{-1}. D-FDOC was rapidly absorbed after oral administration (mean K_a = 0.52 h^{-1}), with peak concentrations in plasma achieved 2 h after dosing and approximately 38% of the oral dose absorbed.

The cumulative urine excretion profiles of D-FDOC versus midpoint of urine collection interval for i.v. and oral doses in the three monkeys are shown in Fig. 4, together with the respective fitted curves. The mean CL_R was 0.18 liter · h^{-1} · kg^{-1}. The CSF concentrations of D-FDOC were 1.9 ± 0.4 μg/ml after i.v. administration and 0.17 and 0.11 μg/ml in two animals after oral administration (Table 2). In the third animal the D-FDOC CSF concentration was below the limit of detection (0.1 μg/ml).

DISCUSSION

Although two antiviral oxathiolane nucleosides were approved by the U.S. Food and Drug Administration for the treatment of HIV, no dioxolane nucleoside has yet been approved. There are several dioxolane nucleosides in clinical development for the treatment of viral infections and cancers, including Amdoxovir (5, 6, 13) and Troxacitabine (12, 28). In the present study, the cellular pharmacology and pharmacokinetics of the dioxolane nucleoside D-FDOC, a potent HIV and hepatitis B virus agent, were studied.

In addition to the D-FDOC-MP, -DP, and -TP, two other peaks were detected in all of the cell extracts. LC/ESI/MS studies in positive mode demonstrated the presence of a metabolite with a molecular weight of 434, corresponding to D-FDOC-DP-ethanolamine. The other unknown metabolite was characterized as D-FDOC-DP-choline. 5′-Diphosphoethanolamine and diphosphocholine may act as intracellular precursors or reservoirs for the active nucleoside triphosphate to reenter the pathway at the monophosphate level (Fig. 5) (15, 30). Cytidine-diphosphocholine contributed about 70 to 80% of phosphatidylcholine (31). The formation of such a liponucleotides has been previously described with other cytidine analogues such as D- and L-ddC and its 5-fluorinated derivatives D- and L-FddC (1, 15). It has been suggested that the peripheral neuropathy observed in humans treated with ddC may be related to the formation of the 5′-diphosphoethanolamine and diphosphocholine metabolites, but this has not been confirmed (10).

D-FDOC accumulated and was rapidly bioconverted in CEM, primary human PBM, and HepG2 cells to the 5′-triphosphate, reaching levels of 6.7 ± 2.3, 2.0 ± 0.1, and 2.8 ± 0.4 pmol/10^6 cells, respectively, within 24 h. No deaminated derivatives were detected with tritiated D-FDOC in these three cell lines, suggesting that this nucleoside is not a substrate for

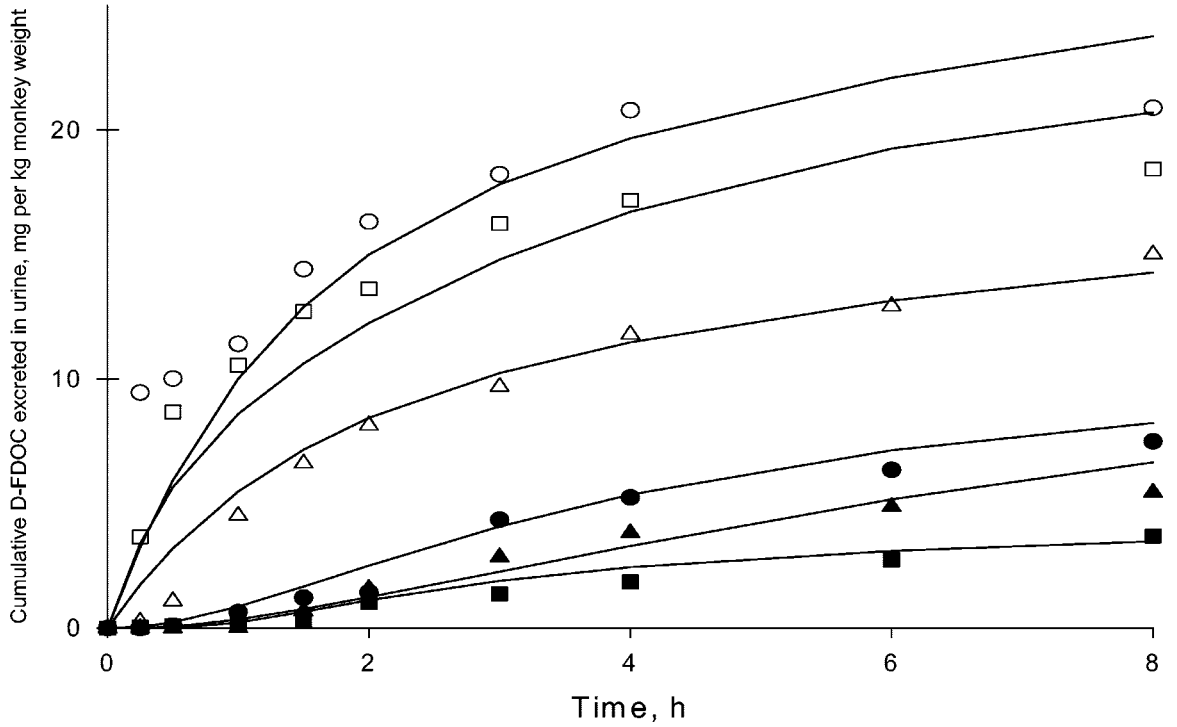

FIG. 4. Observed (symbols) and model predicted (lines) cumulative renal excretion versus time profiles in rhesus monkeys after the administration of 33.3 mg of compound/kg by the i.v. (open symbols) and oral (solid symbols) routes.

cytidine deaminase. CEM cells reached plateau levels of D-FDOC-TP within 8 h, whereas primary human PBM and HepG2 cells failed to reach plateau values within 24 h.

D-FDOC-DP-ethanolamine and choline derivatives reached high levels over a 24-h period and accounted for 54 to 64% of the total phosphates in all cell lines. The precise role of the various nucleoside transporters in the accumulation of D-FDOC was not determined.

The intracellular half-lives of D-FDOC-TP in PBM and HepG2 cells were 5.7 ± 1.4 and 2.7 ± 0.8 h, respectively. Although D-FDOC-TP's half-life in both cell lines was not long, the intracellular concentration of D-FDOC-TP remained

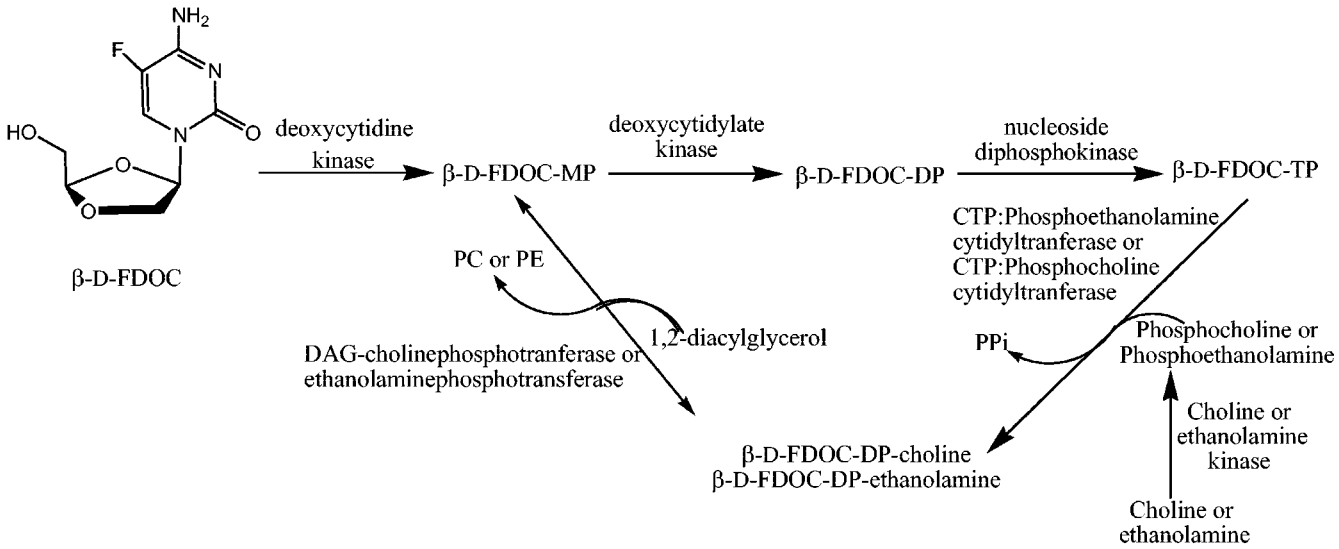

FIG. 5. Proposed pathway for β-D-FDOC-DP-choline and ethanolamine (adapted from Martin et al. [15] with the permission of the publisher). The enzyme and pathway were assumed to be similar to those determined by Martin et al. PS, phosphatidylcholine; PE, phosphatidylethanolamine; PPi, inorganic pyrophosphate; DAG, 1,2-diacylglycerol.

above the IC_{50} for the HIV-1 RT for up to 24 h after removal of the drug from cell cultures (11, 22). Previous studies reported a biological half-life of D-FDOC of >18 h in human T (MT-2) cells that was comparable to Reverset (D-D4FC), a related nucleoside currently in phase IIb clinical trials (S. Erickson-Viitanen, unpublished data) (8, 21, 25). These half-lives, coupled with the low IC_{50} value for D-FDOC in HIV-1 RT, lend support to the possibility of a once-daily dosing regimen

The enzyme thymidine phosphorylase catalyzes the reversible phosphorolysis of several natural and synthetic pyrimidine nucleoside, resulting in cleavage of glycosidic bonds. Susceptibility to this enzyme could adversely influence drug efficacy and metabolism (4, 17). For example, cleavage by this enzyme is believed responsible for the <50% recovery of intact 3′-deoxy-2′,3′-didehydrothymidine in human urine (20, 23). The studies with *E. coli* thymidine phosphorylase enzyme indicate that D-FDOC, like most cytidine analogs, is not a substrate for this enzyme.

D-FDOC, administered i.p. in Swiss mice for 6 days at doses between 3.3 and 100 mg/kg per day, did not result in symptoms of overt toxicity. However, more comprehensive studies involving other species and prolonged dosing intervals may be warranted (27).

A two-compartment open pharmacokinetic model adequately described the plasma and urine concentration profiles for the i.v. and oral doses in rhesus monkeys. D-FDOC was rapidly absorbed after oral administration ($K_a = 0.52 \pm 0.32$ [mean ± the standard deviation]) and had an acceptable oral bioavailability ($F = 0.38 \pm 0.10$). The mean of observed C_{max} and T_{max} values were 7.94 ± 1.46 μg/ml and 2.0 h, respectively. The concentration of D-FDOC in the CSF samples of rhesus monkeys was higher than the EC_{90} value (0.26 μM) against $HIV\text{-}1_{LAI}$ after i.v. (6.92 to 10.16 μM) as well as oral doses (in two monkeys, 0.48 and 0.74 μM) (Table 2), which is higher than other nucleoside RT inhibitors (2, 3). Approximately 72% of the absorbed dose was recovered unchanged in the urine after oral administration in monkeys (CL_R/CL_T). The CL_T value of 0.25 liter · h^{-1} · kg^{-1} for D-FDOC was comparatively low relative to the reported hepatic plasma and renal flow rates of 1.26 and 0.9 liter · h^{-1} · kg^{-1}, respectively, in monkeys (9), but was similar to that of L-2′-Fd4C in rhesus monkeys (0.25 liter · h^{-1} · kg^{-1}) (3). The average CL_R of D-FDOC approached the glomerular filtration rate in rhesus monkeys (0.19 compared to L-2′-Fd4C, 0.2 liter · h^{-1} · kg^{-1}), a finding suggestive of elimination by passive renal filtration (Table 2). The steady-state volume of distribution (V_{ss}) of D-FDOC was similar to that of L-2′-Fd4C (0.96 versus 1.09 liter · kg^{-1}), a finding indicative of a moderate tissue distribution.

The favorable pharmacokinetic profile of D-FDOC in rhesus macaques, an acceptable oral bioavailability, the absence of toxicity in human derived cell lines and in mice, and the antiviral activity observed in vitro warrant further development of D-FDOC as a potential antiviral agent.

ACKNOWLEDGMENTS

This study was supported in part by the Department of Veterans Affairs (R.F.S.) and by NIH grants AI-32351 (C.K.C. and R.F.S.), 2P30-AI-50409 (R.F.S.), and RR00165 (H.M.). B.H.S. is supported by a supplement of NIH grant R37-AI-41980.

REFERENCES

1. **Arner, E. S. J., and S. Eriksson.** 1993. Deoxycytidine and 2′,3′-dideoxycytidine metabolism in human monocytes-derived macrophages. Biochem. Biophys. Res. Commun. **197:**1499–1504.
2. **Asif, G., S. J. Hurwitz, G. Gumina, C. K. Chu, H. M. McClure, and R. F. Schinazi.** 2005. Pharmacokinetics of the antiviral agent β-L-3′-fluoro-2′,3′-didehydro-2′,3′-dideoxycytidine in rhesus monkeys. Antimicrob. Agents Chemother. **49:**560–564.
3. **Chen, H., B. Pai, S. J. Hurwitz, C. K. Chu, Y. Glazkova, H. M. McClure, M. Feitelson, and R. F. Schinazi.** 2003. Antiviral activity and pharmacokinetics of 1-(2,3-dideoxy-2-fluoro-β-L-glyceropentenofuranosyl)cytosine. Antimicrob. Agents Chemother. **47:**1922–1928.
4. **Cretton, E. M., Z. Zhou, L. B. Kidd, H. M. McClure, S. Kaul, M. J. M. Hitchcock, and J.-P. Sommadossi.** 1993. In vitro and in vivo disposition and metabolism of 3′-deoxy-2′,3′-didehydrothymidine. Antimicrob. Agents Chemother. **37:**1816–1825.
5. **De Clercq, E.** 2004. HIV-chemotherapy and prophylaxis: new drugs, leads and approaches. Int. J. Biochem. Cell Biol. **36:**1800–1822.
6. **Furman, P. A., J. L. Jeffrey, L. L. Kiefer, J. Y. Feng, K. S. Anderson, K. Borroto-Esoda, E. Hill, W. C. Copeland, C. K. Chu, J.-P. Sommadossi, I. Liberman, R. F. Schinazi, and G. R. Painter.** 2001. Mechanism of action of 1-β-D-2,6-diaminopurine dioxolane, a prodrug of the human immunodeficiency virus type 1 inhibitor 1-β-D-dioxolane guanosine. Antimicrob. Agents Chemother. **45:**158–165.
7. **Gabrielsson, J., and D. Weiner.** 1997. Pharmacokinetics and pharmacodynamic data analysis, 2nd ed. Apotekarsocieteten, Stockholm, Sweden.
8. **Gelenziunas, R., K. Gallagher, H. Zhang, L. Bacheler, S. Garber, J.-T. Wu, G. Shi, M. J. Otto, R. F. Schinazi, and S. Erickson-Viitanen.** 2003. HIV-1 resistance profile of the novel nucleoside reverse transcriptase inhibitor β-D-2′,3′-dideoxy-2′,3′-didehydo-5-fluorocytidine (Reverset™). Antivir. Chem. Chemother. **14:**49–59.
9. **Gerlowski, L. E., and P. K. Jain.** 1983. Physiologically based pharmacokinetic modeling; principles and applications. J. Pharm. Sci. **72:**1103–1127.
10. **Hao, Z., E. E. Stowe, G. Ahluwalia, D. C. Baker, A. K. Hebbler, C. Chisena, S. M. Musser, J. A. Kelley, C.-F. Perno, D. G. Johns, and D. A. Cooney.** 1993. Characterization of 2′,3′-dideoxycytidine diphosphocholine and 2′,3′-dideoxycytidine diphosphoethanolamine. Drug Metab. Dispos. **21:**738–744.
11. **Hernandez-Santiago, B., T. Beltran, S. J. Hurwitz, C. K. Chu, D. C. Liotta, and R. F. Schinazi.** 2002. Cellular pharmacology of β-D-dioxolane-5-fluorocytosine in human cells. Antivir. Res. **56:**53.
12. **International, L. A.** 2003. Troxacitabine: BCH 4556, SPD 758, Troxatyl. Drugs R. D. **4:**264–268.
13. **Jeffrey, J. L., J. Y. Feng, C. C. Qi, K. S. Anderson, and P. A. Furman.** 2003. Dioxolane guanosine 5′-triphosphate, an alternative substrate inhibitor of wild-type and mutant HIV-1 reverse transcriptase. Steady state and pre-steady state kinetic analyses. J. Biol. Chem. **278:**18971–18979.
14. **Mao, S., M. Bouygues, C. Welch, M. Biba, J. Chilenski, R. F. Schinazi, and D. C. Liotta.** 2004. Synthesis of enantiomerically pure D-FDOC, an anti-HIV agent. Bioorg. Med. Chem. Lett. **14:**4991–4994.
15. **Martin, L. T., A. Faraj, R. F. Schinazi, G. Gosselin, C. Mathé, J.-L. Imbach, and J.-P. Sommadossi.** 1997. Effect of stereoisomerism on the cellular pharmacology of β-enantiomers of cytidine analogs in Hep-G2 cells. Biochem. Pharmacol. **53:**75–87.
16. **Miller, M. D.** 2004. K65R, TAMs and tenofovir. AIDS Rev. **2:**22–33.
17. **Niedzwicki, J. G., M. H. el Kouni, S. H. Chu, and S. Cha.** 1983. Structure-activity relationship of ligands of the pyrimidine nucleoside phosphorylases. Biochem. Pharmacol. **32:**399–415.
18. **Paff, M. T., D. R. Averett, K. L. Prus, W. H. Miller, and D. J. Nelson.** 1994. Intracellular metabolism of (−)- and (+)-*cis*-5-fluoro-1-[2-(hydroxymethyl)-1,3-oxathiolan-5-yl]cytosine in HepG2 derivative 2.2.15 (subclone P5A) cells. Antimicrob. Agents Chemother. **38:**1230–1238.
19. **Rothman, R. E.** 2004. Current Centers for Disease Control and Prevention guidelines for HIV counseling, testing, and referral: critical role of and a call of action for emergency physicians. Ann. Emerg. Med. **44:**31–42.
20. **Schinazi, R. F., D. F. Boudinot, K. J. Doshi, and H. M. McClure.** 1990. Pharmacokinetics of 3′-fluoro-3′-deoxythymidine and 3′-deoxy-2′,3′-didehydrothymidine in rhesus monkeys. Antimicrob. Agents Chemother. **34:**1214–1219.
21. **Schinazi, R. F., J. Mellors, H. Bazmi, S. Diamond, S. Garber, K. Gallagher, R. Gelenziunas, R. Klabe, M. Pierce, M. Rayner, J.-T. Wu, H. Zhang, J. Hammond, L. Bacheler, D. J. Manion, M. J. Otto, L. J. Stuyver, G. Trainor, D. C. Liotta, and S. Erickson-Viitanen.** 2002. DPC 817: a cytidine nucleoside analog with activity against zidovudine- and lamivudine-resistant viral variants. Antimicrob. Agents Chemother. **46:**1394–1401.
22. **Schinazi, R. F., J. Mellors, S. Erickson, J. Mathew, U. Parikh, P. Sharma, M. Otto, Z. Yang, C. K. Chu, and D. C. Liotta.** 2002. D-FDOC: a dioxolane pyrimidine nucleoside with activity against common nucleoside-resistant HIV-1. Antivir. Ther. **7:**S15.
23. **Schinazi, R. F., A. Peck, and J.-P. Sommadossi.** 1992. Substrate specificity of *Escherichia coli* thymidine phosphorylase for pyrimidine nucleosides with

anti-human immunodeficiency virus activity. Biochem. Pharmacol. **44:**199–204.

24. **Sharma, P. L., V. Nurpeisov, B. Hernandez-Santiago, T. Beltran, and R. F. Schinazi.** 2004. Nucleoside inhibitors of human immunodeficiency virus type 1 reverse transcriptase. Curr. Top. Med. Chem. **4:**895–921.
25. **Stuyver, L. J., T. R. McBrayer, D. Schurmann, I. Kravec, A. Beard, L. Cartee, R. F. Schinazi, A. de la Rosa, R. L. Murphy, and M. J. Otto.** 2004. Potent antiviral effect of Reverset in HIV-1-infected adults following a single oral dose. Antivir. Ther. **9:**529–536.
26. **Stuyver, L. J., T. Whitaker, T. R. McBrayer, B. I. Hernandez-Santiago, S. Lostia, P. M. Tharnish, M. Ramesh, C. K. Chu, R. Jordan, J. Shi, S. Rachakonda, K. A. Watanabe, M. J. Otto, and R. F. Schinazi.** 2003. Ribonucleoside analogue that blocks replication of bovine viral diarrhea and hepatitis C viruses in culture. Antimicrob. Agents Chemother. **47:**244–254.
27. **Tennant, B. C., B. H. Baldwin, L. A. Graham, M. A. Ascenzi, W. E. Hornbuckle, P. H. Rowland, I. A. Tochkov, A. E. Yeager, H. N. Erb, J. M. Colacino, C. Lopez, J. A. Engelhardt, R. R. Bowsher, F. C. Richardson, W. Lewis, P. J. Cote, B. E. Korba, and J. L. Gerin.** 1998. Antiviral activity and toxicity of fialuridine in the woodchuck model of hepatitis B virus infection. Hepatology **28:**179–191.
28. **Townsley, C. A., K. Chi, D. S. Ernst, K. Belanger, I. Tannock, G. A. Bjarnason, D. Stewart, R. Goel, J. D. Ruether, L. L. Siu, J. Jolivet, L. McIntosh, L. Seymour, and M. J. Moore.** 2003. Phase II study of troxacitabine (BCH-4556) in patients with advance and/or metastatic renal cell carcinoma: a trial of National Cancer Institute of Canada-Clinical Trials Group. J. Clin. Oncol. **21:**1524–1529.
29. **Van Rompay, K. K. A., T. B. Matthews, J. Higgins, D. R. Canfiled, R. P. Tarara, M. A. Wainberg, R. F. Schinazi, N. C. Pedersen, and T. W. North.** 2002. Virulence and reduced fitness of simian immunodeficiency virus with the M184V mutation in reverse transcriptase. J. Virol. **76:**6083–6092.
30. **Voet, D., and J. G. Voet.** 1990. Lipid metabolism, p. 618–677. *In* J. Stiefel (ed.), Biochemistry. John Wiley & Sons, Inc., New York, N.Y.
31. **Yao, Z., and D. Vance.** 1988. The active synthesis of phosphatidylcholine is required for a very low density lipoprotein secretion from rat hepatocytes. J. Biol. Chem. **263:**2998–3004.